CARBON 47 (2009) 1292–1296

available at www.sciencedirect.com

ScienceDirect

journal homepage: www.elsevier.com/locate/carbon

Selective destruction of individual single walled carbon nanotubes by laser irradiation

*Bardia Zandian, Rajay Kumar, Jesse Theiss, Adam Bushmaker, Stephen B. Cronin**

Electrical Engineering Department, University of Southern California, Los Angeles, California 90089, United States

ARTICLE INFO

Article history:
Received 15 August 2008
Accepted 8 January 2009
Available online 14 January 2009

ABSTRACT

We demonstrate selective burnout of individual carbon nanotubes that are electronically resonant with the incident laser energy. Raman spectroscopy and atomic force microscopy are used to quantify the burnout of nanotubes. The threshold laser power for rapid burnout is found to occur between 0.4 and 0.9 W/μm^2. At lower laser powers of 80 mW/μm^2, the burnout depends linearly on time, over tens of minutes. Non-resonant nanotubes could not be burned out even with high laser power or long exposure times. This preferential burnout of resonant nanotubes demonstrates the possibility of selective removal of metallic nanotubes from an inhomogeneous sample.

1. Introduction

Selective removal of metallic carbon nanotubes remains one of the most formidable challenges currently limiting the practical application of nanotubes as electronic circuit elements. The main difficulty in scaling up carbon nanotube devices into large arrays lies in the inhomogeneity of nanotube samples, which contain both metallic and semiconducting nanotubes. The metallic nanotubes invariably spoil the device performance, as they tend to short-circuit the behavior of the semiconducting nanotubes. Many techniques have been investigated for separating metallic and semiconducting nanotubes including precipitation of single walled carbon nanotubes (SWCNTs) non-covalently functionalized with octadecylamine (ODA) in tetrahydrofuran (THF) [1], selective functionalization with diazonium salts [2], centrifugation after addition of diluted bromine [3], electrophoresis [4,5], and chromatography [6,7]. Others have tried preferential growth of semiconducting SWCNTs by controlling the conditions of the growth process, chemicals, catalysts, and substrate [8]. A third approach is to preferentially destroy metallic SWCNTs while leaving the semiconducting SWCNTs intact.

It has been shown that light irradiation can enhance the oxidation of SWCNTs treated with H_2O_2. This method has been used for diameter-selective removal of SWCNTs [9]. Solution-phase ozonolysis of SWCNTs has also been used for diameter selectivity in SWCNTs [10]. Laser-resonance chirality-selective removal of SWCNTs by intense laser irradiation has been demonstrated on macroscopic quantities of nanotubes [11]. Huang et al. [12] performed bulk measurements of SWCNTs functionalized with 4-brominebenzenediazonium [13], showing that metallic carbon nanotubes can be selectively destroyed due to the different rates of photolysis-assisted oxidation. All of these previous experiments were performed on large ensembles of SWCNTs. Zhang et al. studied laser heating of nanotubes by monitoring the Raman spectra of individual suspended SWCNTs at relatively low laser powers (1 mW/μm^2) [14], which can generally be neglected for SWCNTs on solid substrates because of the strong thermal coupling to the substrate. Kumar et al. showed laser burnout of individual carbon nanotubes by surface plasmon resonant nanoparticles [15].

In this paper, we present a method that requires no chemical functionalization of the nanotubes, and relies solely on the selective heating of the resonant nanotubes. We demonstrate

* *Corresponding author:* Fax: +1 213 740 8677.
E-mail address: scronin@usc.edu (S.B. Cronin).
0008-6223/$ - see front matter
doi:10.1016/j.carbon.2009.01.012

selective burnout of individual carbon nanotubes based on their electronic transition energies. The threshold laser power for burnout is quantified for a number of resonant nanotubes, together with the time-dependence of the burnout process. The laser destruction is corroborated with AFM images.

2. Experimental

2.1. Sample Preparation

SWCNTs synthesized by the arc discharge method are deposited from a sonicated dichloroethane solution onto a Si substrate coated with a 1 μm layer of SiO_2 [16]. A numbered grid of Cr/Au is patterned on the substrate using electron beam lithography, allowing correlation of micro-Raman spectroscopy with atomic force microscopy (AFM). A 532 nm spectra-physics solid state laser is used for both sampling and burning the target SWCNTs. The laser beam is focused and collimated through a Leica DMLM microscope with a 50X and a 100X objective lens. A Renishaw in Via Raman microspectrometer is used to identify resonant nanotubes and record their position relative to the numbered fiducial grid. Atomic force microscopy was performed in a Digital Instruments, Dimension 3100. After a resonant SWCNT is detected, AFM images are collected to determine the bundle diameter and confirm that it is an individual nanotube bundle, isolated from other nanotubes and debris on the substrate. The G-band Raman peak, appearing around 1590 cm^{-1}, was used to quantify the laser-induced destruction of the nanotubes.

3. Experimental results and discussion

Fig. 1 shows the relative change in the G-band Raman intensity of an isolated carbon nanotube bundle after successive exposures with increasing laser power. During the high laser power exposures, samples were irradiated for a duration of 120 s. Spectra were collected at a low laser power of 2 mW/μm^2 for 180 s to avoid any additional heating and/or burnout. The drop in Raman intensity as the laser power is increased with each exposure indicates the extent to which the nanotubes are burnt out. We begin to see significant burnout at laser power densities of 0.2 W/μm^2. Above 0.6 W/μm^2, the slope of the Raman intensity changes dramatically. This indicates a regime where the nanotube is completely burnt out in the region of the focused laser spot and slight burnout continues to occur in the tails of the Gaussian beam. AFM imaging shows the diameter of this bundle to be 2.3 nm. Further details of this nanotube are given in data set 6 of Table 1.

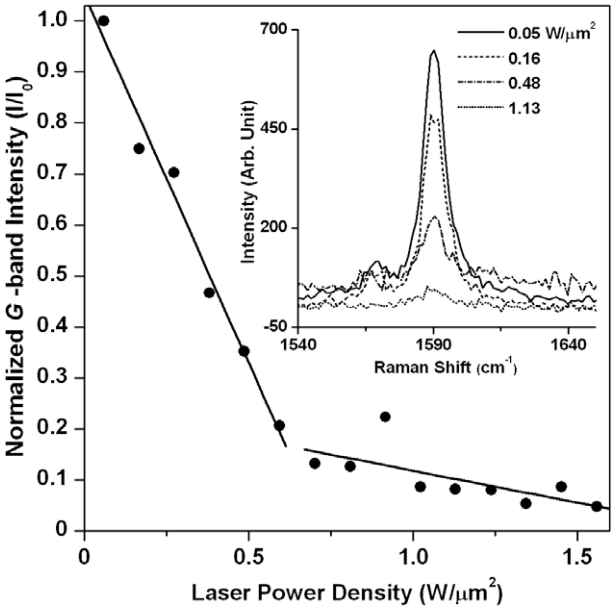

Fig. 1 – Normalized G-band Raman intensity of an individual SWCNT bundle as a function of laser power exposure. The inset shows the raw Raman data from the nanotube.

Fig. 2 shows an AFM image of a carbon nanotube bundle before and after being burned out with a 160 mW/μm^2 laser spot. The laser spot was placed at several different locations along the length of the nanotube, which resulted in the nanotube being burnt out in these regions. The white circles in the figure indicate the approximate size and location of the laser spot when the nanotube was irradiated. The diameter of this bundle was measured by AFM to be 5 nm, which is expected to contain approximately 11 nanotubes. The bundle contains only one resonant nanotube that has a radial breathing mode (RBM) at $\omega_{RBM} = 193\ cm^{-1}$, which corresponds to a diameter of 1.28 nm from the relation $\omega_{RBM} = 204/d_t + 27$ [17]. The large enhancement in the light absorption of nanotubes enables the selective burn out of nanotubes that are resonant with the laser energy. For non-resonant nanotubes, no such burnout is observed. Fig. 2c shows data from a power dependent laser exposure showing destruction of the nanotube as the laser power is increased. The linear trend line shown in Fig. 2c is given by $y = -0.988x + 0.909$. While the AFM images provide fairly convincing evidence for nanotube burnout, we must consider the possibility of non-thermal effects, such as charge injection from the substrate and neighboring nanotubes, causing a change in the resonant nanotube intensity [18]. In this case, charge transfer should affect the entire length of the nanotube. However, we do not observe a drop in the Raman intensity away from the local region of burnout on these nanotubes, enabling us to rule out such mechanisms.

We also investigate the time-dependence of the nanotube burnout process at a relatively low, constant laser power. Fig. 3 shows the normalized G-band Raman intensity of a SWCNT after successive irradiations at a power density of 80 mW/μm^2. The resonant nanotube diameter, as determined from the AFM image, is 1.3 nm, indicating that this is likely an individual carbon nanotube rather than a bundle. Raman spectra, again, were taken at lower laser power (2 mW/μm^2), after re-aligning the laser spot to eliminate the effect of sample drift on the measurement. We observe the G-band Raman intensity to decrease linearly with time on the scale of tens of minutes. The trend line shown in the figure is given by $y = -0.006x + 0.896$.

By comparing the high power and low power burnouts, we find that the destruction observed after less than 20 s of exposure to 1000 mW/μm^2 of laser power is much more significant than the destruction caused by 2 h of exposure to 80 mW/μm^2. After studying different SWCNTs, it can be concluded

Table 1 – Comparison of data from different laser exposures on different nanotube samples, listing the radial breathing mode (for nanotubes exhibiting one in their spectra), nanotube and bundle diameters as determined from the RBM and AFM, the initial G-band Raman intensity, and the threshold laser power for 50% and 80% reduction in Raman intensity.

Data set	RBM (cm^{-1})	Diameter from RBM (nm)	Diameter from AFM (nm)	Initial G-band intensity (counts)	Threshold laser power for 50% reduction in Raman intensity ($W/\mu m^2$)	Threshold laser power for 80% reduction in Raman intensity ($W/\mu m^2$)
1	181	1.32	2.6	3281	0.70	1.24
2	181	1.32	2.6	5267	0.38	0.92
3	181	1.32	2.6	1589	0.81	1.88
4	181	1.32	2.6	6094	0.91	2.60
5	–	–	1.2	650	0.38	1.77
6	–	–	2.3	1170	0.38	0.60
7	–	–	1.1	3402	0.38	0.91
8	–	–	3.7	2335	0.81	1.30
9	193	1.28	5	763	0.43	0.70

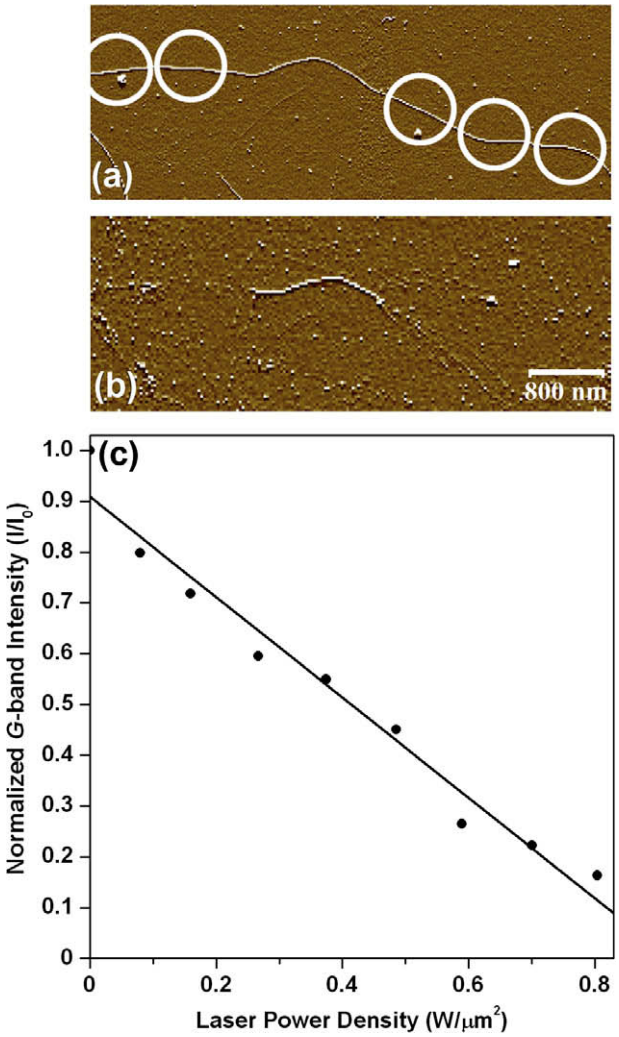

Fig. 2 – Atomic force microscope (AFM) images of a carbon nanotube (a) before and (b) after being burned out by a 160 $mW/\mu m^2$ focused laser spot. The white circles in the image indicate the size and location of the laser spot when the nanotube was irradiated. Details of this nanotube are given in data set 9 of Table 1. (c) Normalized G-band Raman intensity plotted as a function of exposure laser power.

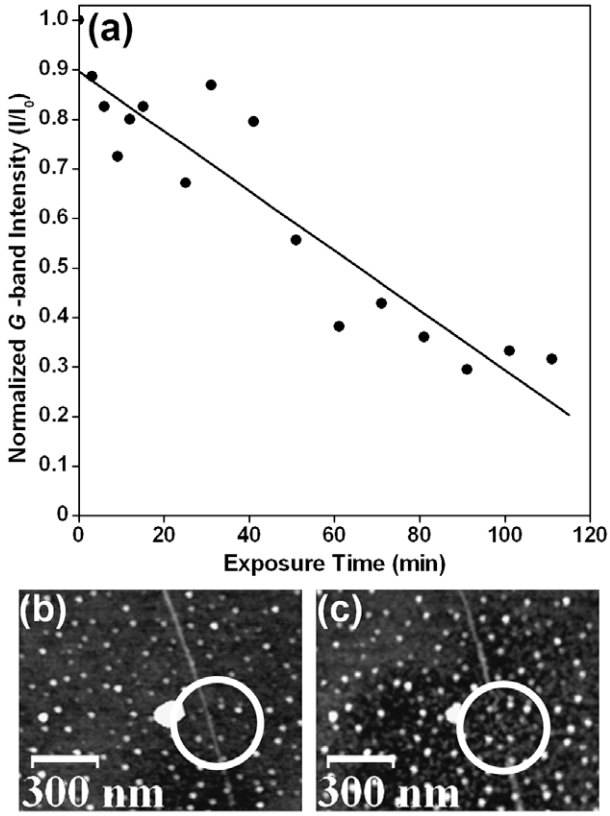

Fig. 3 – (a) G-band Raman intensity plotted as a function of laser exposure time at a power of 80 $mW/\mu m^2$. AFM image of the target SWCNT (b) before and (c) after a 111 min laser exposure.

that the destruction is more strongly dependent on laser power than on exposure time. The *D*-band Raman intensity of carbon nanotubes gives a relative indication of the amount of disorder and defects in the nanotube. In some cases there was an initial increase in the *D*-band as the burnout took place and in many other cases the *D*-band showed a reduction with irradiation, however, no consistent trend was observed.

Table 1 shows a compilation of the laser-induced burnout data of several carbon nanotubes, listing values for the nanotube diameter, initial G-band Raman intensity (measured with a 532 nm laser at 2 mW/μm^2 for a 180 s collection time), and threshold laser power for producing a 50% and 80% reduction in the Raman intensity with an exposure time of 20 s. The initial G-band Raman intensity gives a relative measure of the strength of the optical resonance. Surprisingly, the threshold laser power for 50% burnout is relatively insensitive to the initial G-band intensity. The large variation in burnout thresholds, and lack of correlation with initial Raman intensity, indicates that the key limiting factor in the burnout of nanotubes lies in their thermal coupling to the substrate rather than the strength of their optical resonance. The strong thermal coupling to the underlying substrate limits the temperatures that can be reached by laser heating. All of the samples used in these measurements were individual isolated SWCNTs or small bundles of SWCNTs. Bundles are distinguished from individual isolated SWCNTs by comparing the AFM-measured diameter with the RBM-determined diameter. All of the bundles in this work are small bundles containing only a handful of nanotubes. Only one resonant nanotube, at most, is present within each bundle. In fact, most of the bundles in this sample were found to be non-resonant. The data presented in Table 1 represents a subset of nanotubes that were carefully selected after surveying a much larger number of nanotubes.

Data sets 1–4 in Table 1 have been collected from different segments of the same nanotube. It is for this reason that these data sets report the same RBM. The variability in initial G-band peak intensities and destruction thresholds can be attributed to slight misalignment of the focused laser spot and inhomogeneity in the thermal coupling to the substrate. This inhomogeneity is an inherent variability in this laser burnout technique. Despite this, we are still able to selectively burn resonant nanotubes, while leaving non-resonant nanotubes intact. Both the time and power dependence of the burnout are very gradual. This gradual burnout process is likely due to the evolution and nucleation of defects, which interact with the occasional oxygen molecule that hits the nanotube under ambient conditions. In this burnout mechanism, non-resonant nanotubes within a bundle are burned out along with the resonant nanotube. While these results demonstrate the principle of selective burnout of resonant nanotubes, practical implementation of this technique should be carried out on an array of individually isolated nanotubes in order to achieve high yields. In this work, the nanotube burn out is performed in air. Here, oxygen burns the carbon exothermically. This leads to thermal gradients and an uncontrollable burn, which is likely the cause of the non-resonant burn out that is observed. Performing the burn out in a water vapor environment would result in an endothermic burn and may lead to more localized burn out, perhaps only on resonance.

4. Conclusions

In conclusion, we demonstrate the preferential destruction of carbon nanotubes based on their electronic transition energies. Several aspects of this burnout process are quantified, including the time and laser power dependence. We find the threshold laser power for burnout to occur between 0.4 and 0.9 W/μm^2. At lower laser powers of 80 mW/μm^2, the burnout depends linearly on time, over tens of minutes. The spatial extent of the burnout is limited to the laser spot size, despite the nanotubes' extremely high thermal conductivity. Bundles containing no resonant nanotubes could not be burnt out even with high laser power or long exposure times. These results support the possibility of selective removal of metallic carbon nanotubes from an inhomogeneous sample, since their resonant electronic transitions are generally separated in energy from those of semiconducting nanotubes. This is important for enriching the semiconducting:metallic ratio in an inhomogeneous sample of carbon nanotubes.

Acknowledgement

This research was supported in part by DOE Award No. DE-FG02-07ER46376.

REFERENCES

[1] Chattopadhyay D, Galeska I, Papadimitrakopoulos F. A Route for Bulk Separation of Semiconducting from Metallic Single-Wall Carbon Nanotubes. J Am Chem Soc 2003;125:3370–5.
[2] Strano M, Dyke C, Usrey M, Barone P, Allen M, Shan H, et al. Electronic Structure Control of Single-Walled Carbon Nanotube Functionalization. Science 2003;301:1519.
[3] Chen Z, Du X, Du M, Rancken C, Cheng H, Rinzler A. Bulk Separative Enrichment in Metallic or Semiconducting Single-Walled Carbon Nanotubes. Nano Lett 2003;3:1245–9.
[4] Krupke R, Hennrich F, Löhneysen H, Kappes M. Separation of Metallic from Semiconducting Single-Walled Carbon Nanotubes. Science 2003;301:344.
[5] Kim W, Usrey M, Strano M. Selective Functionalization and Free Solution Electrophoresis of Single-Walled Carbon Nanotubes: Separate Enrichment of Metallic and Semiconducting SWNT. Chem Mater 2007;19:1571–6.
[6] Heller D, Mayrhofer R, Baik S, Grinkova Y, Usrey M, Strano M. Concomitant Length and Diameter Separation of Single-Walled Carbon Nanotubes. J Am Chem Soc 2004;126:14567–73.
[7] Chen Y, Wei L, Wang B, Lim S, Ciuparu D, Zheng M, et al. Low-Defect, Purified, Narrowly (n,m)-Dispersed Single-Walled Carbon Nanotubes Grown from Cobalt-Incorporated MCM-41. ACS Nano 2007;1:327–36.
[8] Ryu K, Badmaev A, Gomez L, Ishikawa F, Lei B, Zhou C. Synthesis of Aligned Single-Walled Nanotubes Using Catalysts Defined by Nanosphere Lithography. J Am Chem Soc 2007;129:10104–5.
[9] Yudasaka M, Zhang M, Iijima S. Diameter-selective Removal of Single-wall Carbon Nanotubes Through Light-assisted Oxidation. Chem Phys Lett 2003;374:132–6.
[10] Banerjee S, Wong S. Demonstration of Diameter-Selective Reactivity in the Sidewall Ozonation of SWNTs by Resonance Raman Spectroscopy. Nano Lett 2004;4:1445–50.
[11] Maehashi K, Ohno Y, Inoue K, Matsumoto K. Chirality Selection of Single-walled Carbon Nanotubes by Laser Resonance Chirality Selection Method. Appl Phys Lett 2004;85:858.

[12] Huang H, Maruyama R, Noda K, Kajiura H, Kadono K. Preferential Destruction of Metallic Single-Walled Carbon Nanotubes by Laser Irradiation. J Phys Chem B 2006;110:7316–20.
[13] Strano M. Probing Chiral Selective Reactions Using a Revised Kataura Plot for the Interpretation of Single-Walled Carbon Nanotube Spectroscopy. J Am Chem Soc 2003;125:16148–53.
[14] Zhang Y, Son H, Zhang J, Kong J, Liu Z. Laser-Heating Effect on Raman Spectra of Individual Suspended Single-Walled Carbon Nanotubes. J Phys Chem C 2007;111:1988–92.
[15] Kumar R, Zhou H, Cronin S. Surface-enhanced Raman Spectroscopy and Correlated Scanning Electron Microscopy of Individual Carbon Nanotubes. Appl Phys Lett 2007;91:223105.
[16] Cronin S, Swan A, Ünlü M, Goldberg B, Dresselhaus M, Tinkham M. Measuring the Uniaxial Strain of Individual Single-Wall Carbon Nanotubes: Resonance Raman Spectra of Atomic-Force-Microscope Modified Single-Wall Nanotubes. Phys Rev Lett 2004;93:167401.
[17] Meyer J, Paillet M, Michel T, Moreac A, Neumann A, Duesberg G, et al. Raman Modes of Index-Identified Freestanding Single-Walled Carbon Nanotubes. Phys Rev Lett 2005;95:217401.
[18] Cronin SB, Barnett R, Tinkham M, Chou SG, Rabin O, Dresselhaus MS, et al. Electrochemical Gating of Individual Single-wall Carbon Nanotubes Observed by Electron Transport Measurements and Resonant Raman Spectroscopy. Appl Phys Lett 2004;84:2052.